Genetic Dissection of Chiari Type I Malformation

Christina Ann Markunas

Advisors: Dr. Allison Ashley-Koch and Dr. Simon Gregory

A. SPECIFIC AIMS

Chiari Type I Malformation (CMI) is characterized by herniation of the cerebellar tonsils through the foramen magnum. Individuals usually present with a range of neurological symptoms in their twenties, although the age of onset is variable and can occur during childhood. CMI is a clinically heterogeneous disorder, as is evident by the variation that exists in the pattern and severity of symptoms, response to surgery, presence of associated conditions, and the extent of tonsillar herniation. Currently, the only treatment for CMI is suboccipital surgical decompression surgery; however, guidelines for treatment and selection of patients for surgery are still not well established. It is thought that the primary defect in CMI is a small posterior fossa (PF) due to an underdeveloped occipital bone. The normal sized cerebellum becomes cramped in the PF resulting in tonsillar herniation. There are several lines of evidence suggesting a genetic component for CMI. These include twin studies showing a higher concordance between monozygotic twins compared to dizygotic twins, familial clustering, and the fact that CMI co-occurs with established genetic syndromes. In addition, a genome-wide linkage screen conducted by our group using 23 multiplex families identified significant evidence for linkage to regions on chromosome 9 and 15 using Affymetrix 10K SNP Chips.

While the findings from our initial linkage screen are encouraging, the linked regions (LOD > 1) on chromosome 9 and 15 are not currently manageable for detailed follow-up due to their size. The region on chromosome 9 spans 40 cM containing 193 known genes and the region on chromosome 15 spans 13 cM containing 71 known genes. We are proposing to expand on the initial linkage work by conducting a larger screen using at least 58 multiplex families, which includes 16 of the families used previously. Currently, we are in a much better position to identify more precise and potentially informative linkage peaks. Since the time of the initial linkage screen, we have more than doubled our initial sample size, which in turn has allowed us to further reduce the clinical heterogeneity across families. In addition, individuals will be genotyped using Illumina Human610 BeadChips, allowing us to more precisely map the disease gene(s) due to the increased genomic coverage. We will also have access to additional clinical information, as well as blood and dura mater samples from affected patients for whole genome expression analysis. These will be used for clinical and biological characterization of CMI patients, thus allowing us to further refine our linkage analysis. Future work will consist of the follow-up of significant linkage peak(s) by fine-mapping, followed by the selection of candidate genes/regions for sequencing.

Specific Aim 1. To perform a qualitative linkage screen using multiplex CMI families. Fifty eight nonsyndromic, multiplex families meeting our inclusion criteria for a qualitative linkage screen have been ascertained to date. We are currently ascertaining additional families for linkage analysis. Eligible families must contain at least two sampled individuals with CMI with or without syringomyelia and the CMI cannot be acquired or syndromic. Individuals will be genotyped using Illumina Human610-Quad BeadChips. Both parametric and nonparametric linkage analysis will be performed to identify regions showing significant evidence for linkage. If important clinical covariates related to CMI subtypes are identified in Specific Aim 2, I will perform an ordered-subset analysis (OSA) to reduce the impact of potential heterogeneity among our families. The 1-LOD score down support intervals will be defined for future follow-up of significant peaks.

Specific Aim 2. To identify CMI subtypes using clinical and biological factors. We anticipate enrolling 50 pediatric patients who are scheduled for decompression surgery with duraplasty. Questionnaires, medical records, cranial morphology measurements from MRIs, and CSF flow findings will be used for clinical characterization of each patient. In addition, I will generate gene expression data from blood and dura mater samples using Illumina HT-12 v3 Expression BeadChips. Clinical and biological features will be used separately to cluster CMI patients into more

homogeneous classes, or subtypes. Comparison of these clustering outcomes will determine if patients with similar clinical features have similar gene expression patterns. Finally, identification of important clinical features will be used to help guide the linkage analysis in Specific Aim 1.

B. BACKGROUND AND SIGNIFICANCE

CMI phenotype

CMI is characterized by herniation of the cerebellar tonsils through the foramen magnum into the cervical canal (1). Individuals are generally considered affected if one tonsil is herniated 5 mm or more or both tonsils are herniated 3 mm or more. Magnetic resonance imaging (MRI) is considered the gold standard for the diagnosis of CMI (Figure 1). CMI patients exhibit a wide range of symptoms, making it difficult to identify which symptoms are directly related to the disease itself. In addition, many of these symptoms are vague and not specific to CMI, resulting in misdiagnoses (2). In a cohort of 265 CMI patients, the ten most frequent symptoms reported included headache (98%), dizziness (84%), difficulty sleeping (72%), weakness of an upper extremity (69%), neck pain (67%), numbness/tingling of an upper extremity (62%), fatigue (59%), nausea (58%), shortness of breath (57%), and blurred vision (57%) (2). Much variability exists in terms of the types and severity of symptoms present. In fact, some patients exhibit no signs or symptoms and obtain a diagnosis incidentally or because a family member was diagnosed.

Figure 1. Sagittal MRI of an individual affected with CMI. The horizontal red line marks the level of the foramen magnum. The vertical red line shows the extent of tonsillar herniation.

CMI is a clinically heterogeneous disorder. This is evident by the variation in symptom presentation, age of onset, presence of associated conditions, and the extent of tonsillar herniation. CMI patients usually present with symptoms in their twenties or thirties (1), although the age of onset can occur at any time even though diagnoses are rarely made before the age of one. An associated condition, syringomyelia, is found in 65-80% of CMI patients (3). This condition occurs when a syrinx, or fluid filled sac, forms within the brain stem or spinal cord (4). Additionally, over two thirds of patients have bony abnormalities of the PF, including platybasia, basilar impression, and enlargement of the foramen magnum (5). Other conditions which may be found in association with CMI include scoliosis, kyphosis, hydrocephalus, and empty sella (1). In addition, a variety of genetic syndromes can co-occur with CMI, such as Achondroplasia, Crouzon syndrome, Klippel-Feil, Paget's disease of the bone, hereditary disorders of connective tissue, and others (3;6). The extent of tonsillar herniation can also be extremely variable and does not have to be symmetric with respect to both tonsils. Previous studies have even suggested that CM0, which is idiopathic syringomyelia with no tonsillar herniation, may have a similar etiology as CMI (7;8).

Epidemiological and Genetic Studies of CMI

Although no well designed prevalence studies for CMI exist, there have been several studies which provide estimates of the prevalence. The first was a retrospective study which examined 22,591 individuals who received MRIs at Johns Hopkins hospital between January 1, 1994 and July 13, 1997 (9). Less than one percent (~1/125) of the study population was diagnosed with CMI, defined as tonsillar herniation exceeding 5 mm (9). Of the 175 individuals diagnosed with CMI, 25 were asymptomatic (~1/900). A separate study estimated the prevalence indirectly based on prevalence estimates of syringomyelia and the fact that it is found in 65-80% of CMI patients (3). They

estimated that 0.08% of the population of the United States was affected with CMI with or without syringomyelia (3). At this time, it is difficult to determine whether the prevalence of CMI has been underestimated due to asymptomatic individuals or whether the prevalence has been overestimated due to the study designs described above.

Although little is known about the genetics of CMI, there are several lines of evidence which suggest a genetic component in at least a subset of nonsyndromic cases. These include twin studies, familial clustering and co-segregation with known genetic syndromes. The largest twin study to date compared three sets of monozygotic twins to three sets of dizygotic twins and found a higher concordance between monozygotic twins compared to dizygotic twins (3). There have also been at least three additional studies which report the concordance between sets of monozygotic twins (10-12) and another study describing a set of monozygotic triplets (13). In general, twins were concordant with respect to the CMI diagnosis, although they were sometimes discordant with respect to the presence of syringomyelia, age of onset, extent of tonsillar herniation, and symptom severity. In addition to twin studies, there is also evidence for familial clustering (1;12;14). In a cohort of 364 symptomatic patients, 43 patients reported that they had at least one close relative with CMI with or without syringomyelia or idiopathic syringomyelia (1). An additional 72 patients reported that they had at least one close relative with symptoms similar to their own (1). The mode of inheritance for CMI appears to be consistent with either autosomal dominant with reduced penetrance, or autosomal recessive (1). In addition, females appear to be three times more likely to be affected than males (1). Finally, there is also evidence that CMI can co-occur with established genetic syndromes, suggesting there may be an underlying genetic link between these disorders (3;6).

Treatment of CMI

Suboccipital surgical decompression is currently the only form of treatment for CMI (15). A typical Chiari surgery involves removing a small portion of the occipital bone, followed by making a “Y” shaped incision in the dura mater from the suboccipital region through the C1 vertebra and then closing the dura with a “V” shaped patch (duraplasty) to expand the subarachnoid space below (Dr. Herbert Fuchs, personal communication). Studies suggest that only 40-60% of patients show improvement of symptoms following decompression surgery (16;17).

Duraplasty, as described above, is often used in conjunction with suboccipital surgical decompression. The dura mater is the outermost meningeal layer and may be involved in the development of CMI. Previous studies reported the presence of a thickened dural band at the craniovertebral junction of CMI patients (18;19). The thickened dural band showed evidence of increased collagen fiber splitting and branching, as well as hyalinosis, calcification, and ossification (18). In addition, hypovitaminosis A has been associated with a CMI-like malformation in lions that is generally accompanied by a thickening of the occipital bone (20;21). Cousins, et al. examined the effects of a vitamin A deficient diet in male Holstein calves and found evidence of dural thickening, an increase in the mucopolysaccharide concentration and total RNA in the dura mater, along with an increase in CSF pressure (22). In addition, vitamin A fed to pregnant hamsters during their 8th day of gestation induced CMI and CMII (23). Retinoic acid (vitamin A) administered to mice at E10.0 resulted in reduced neural crest-derived meninges and inhibited ossification of the parietal bones and interparietal bone (portion of occipital bone which undergoes intramembranous ossification); ectopic cartilage was formed in place of the bone (24). The dura mater also plays a role in craniosynostosis, which can co-occur with CMI. Craniosynostosis, the premature fusing of cranial sutures, is thought to be caused by aberrant dura-derived paracrine signals that play an essential role in determining suture fate (25). In response to the growing brain, the dura mater sends signals to the sutures to increase bone production which results in growth of the cranial vault (26).

Cranial Morphology and Causal Theories

There is a substantial amount of literature which compares measurements of the PF region in CMI cases versus controls. A recent paper reviewed the findings from eight studies (27). Across all eight studies, the clivus or basiocciput was significantly shorter in cases compared to controls, although in one study the finding was not significant for women and in another study it was only significant when comparing CMI patients who also had basilar invagination (27). Out of five studies that examined the length of the supraocciput, all found that it was shorter in CMI patients, although only two studies found the difference to be significant (27). Three studies examined PF area and all found that it was significantly smaller in cases compared to controls (27). In addition, three studies examined PF volume and all found that it was smaller in cases compared to controls, but only one study found the difference to be significant (27). In one of those studies, the ratio of the PF brain volume to the PF cranial volume was significantly different, even though the PF volume alone was not significantly different (28). Out of the five studies which examined the tentorial angle, all reported that the angle was larger in cases compared to controls, and four identified this difference as being significant (27). Five of the eight studies examined neural structures, such as the brainstem and cerebellum, and all found these to be normal (27).

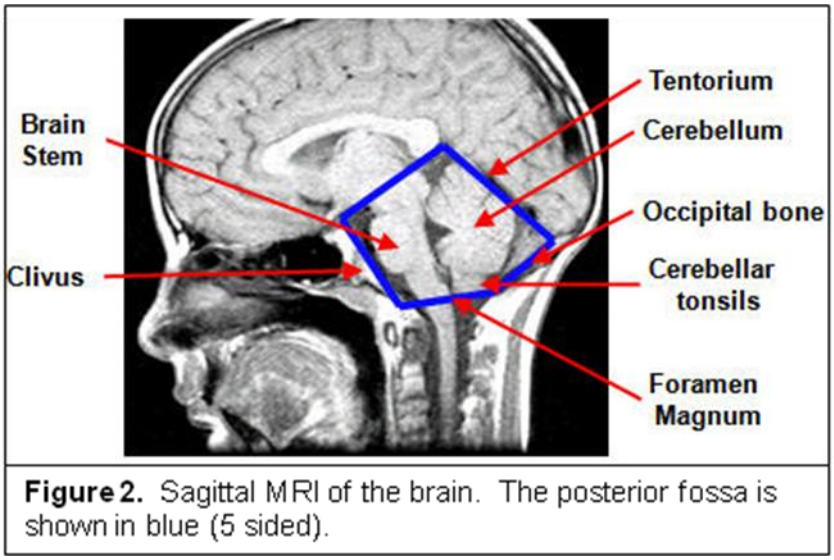

Figure 2. Sagittal MRI of the brain. The posterior fossa is shown in blue (5 sided).

As illustrated above, one of the most consistent MRI findings in CMI patients is a shorter basiocciput or clivus. A short basiocciput or clivus can result from two different mechanisms: an early developmental defect leading to an underdeveloped bone, and/or the premature fusion of the sphenooccipital synchondrosis, which is the cartilaginous joint between the basiocciput and basisphenoid bone that normally closes between 16 and 20 years of age (27). CMI is thought to be caused by an underdeveloped occipital bone which originates from the paraxial mesoderm (23;28). This results in a PF which is too small and shallow to accommodate the normal sized cerebellum (23;28). Herniation of the cerebellar tonsils and an upward shift of the tentorium are thought to occur secondarily (28).

Significance

There is a significant amount of evidence which suggests a genetic component of CMI, although no genes have been identified to date. We are in a unique position to perform this type of study, as we have the largest collection of CMI families in the world. By restricting our study to a set of clinically homogeneous families, as well as using additional clinical and biological information to guide our linkage analysis, we are now in a better position to identify major genes which play a role in the development of CMI. In addition, our study should provide us with additional information regarding biologically relevant subtypes which may lead to research focused at the development of more specific treatment plans for groups of patients. Although our study focuses on the identification of susceptibility genes in a small group of families, information gleaned from this study will likely provide information regarding the biological mechanisms that may be involved in additional families, as well as in sporadic cases.

C. PRELIMINARY DATA

I. Preliminary Data for Specific Aim 1

Qualitative Linkage Screen

In 2006, an initial linkage screen was performed using 23 Caucasian multiplex families containing 67 sampled individuals affected with CMI with or without syringomyelia (29). Individuals were genotyped by Translational Genomics using the whole-genome Affymetrix 10K SNP Chip (TGen, Phoenix, AZ). PEDCHECK (30) was used to identify Mendelian inconsistencies and RELPAIR (31;32) was used to confirm familial relationships. In addition, markers with a genotyping efficiency less than 85% or heterozygosity less than 0.05 were removed from the analysis. Markers were also removed due to inter-marker linkage disequilibrium (LD) (r^2>0.16), which can inflate the type I error rate in multipoint linkage analysis when one or both parents are missing (33).

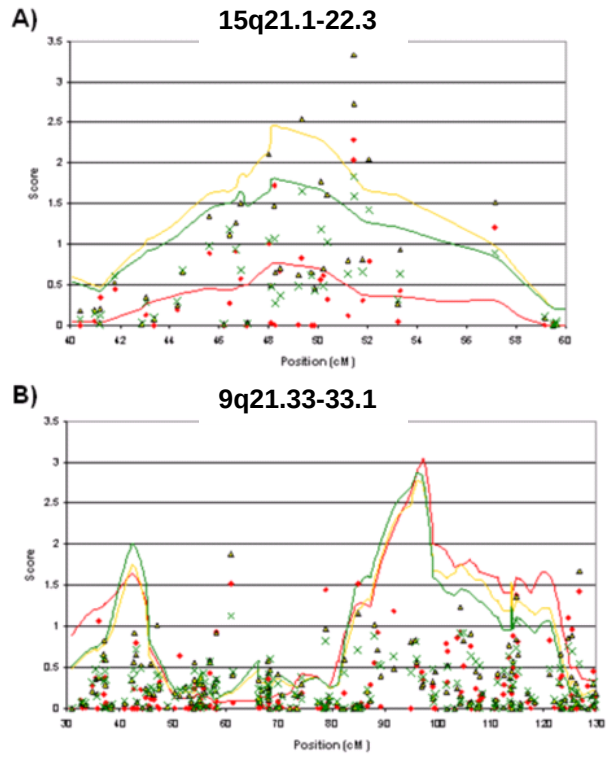

Figure 3. Genomic regions showing the most significant evidence for linkage. Red diamond and line= 2 point and multipoint under a parametric model, HLOD score; Yellow triangle and line= 2 point and multipoint under an exponential model, Spairs LOD; and Green "X" and line= 2 point and multipoint under a linear model, Spairs LOD.

Both parametric and nonparametric linkage analysis was performed since the underlying genetic model for CMI is unknown. For the parametric linkage analysis, model assumptions included an autosomal dominant mode of inheritance, prevalence of 0.0005, and 80% penetrance. For the nonparametric analysis, the S_{pairs} statistic (34;35) was used, as well as both the linear and exponential models (36). ALLEGRO v1.2 (35) was used to perform all analyses, including two-point and multipoint.

Significant evidence for linkage was identified on regions of chromosome 9 and 15 (Figure 3). The highest two-point LOD score (3.332-Exponential model) was found on chromosome 15 (Figure 3- A). An additional four markers in this location had LOD scores exceeding 2 (2 markers- Parametric model, 2 markers- Exponential model). In addition, multipoint analysis using an exponential model produced a linkage peak approaching 2.5 near the region which produced the high two-point LOD scores.

The highest multipoint score was seen on chromosome 9. The multipoint analyses using the parametric model (3.05), exponential model (2.77), and linear model (2.86) all peaked between the same markers, rs1000735 and rs2895201. No significant two-point LOD scores were obtained in this region, regardless of the model used. Another small peak approaching a LOD score of 2 was obtained a bit upstream from the main region of interest on chromosome 9.

Heritabilities of Cranial Morphology Measurements

MRI scans collected on a subset of individuals from families included in the linkage screen, as well as additional families that were not eligible for the linkage screen were used to take a series of measurements of the PF region in affected and unaffected individuals. Under the supervision of a board certified radiologist (Dr. David Enterline), two trained researchers took measurements from T1-weighted sagittal (Figure 4) and axial MRI scans. On average, measurements between researchers were highly correlated (0.91 for herniations, 0.79 for other measures taken from the midline of a sagittal scan, and 0.96 for volume). Herniation of the left and right tonsils was measured on a line drawn from the tips of the cerebellar tonsils perpendicularly to the foramen magnum on a sagittal image to the left and right of the midline, respectively. Basal angle was measured as the angle between a line extending from the basion to the center of the sella turcica and a line extending from the sella turcica to the nasion. The clivus was measured from the basion to the top of the dorsum sella. The foramen magnum was measured from the basion to the opisthion. The supraoccipital bone was measured from the opisthion to the center of the internal occipital protuberance. The tentorium was measured from the center of the internal occipital protuberance to just posterior of the vein of Galen. Cranial volume calculations were estimated from a series of axial MRIs taken from the foramen magnum to the top of the skull. The area of the PF and total cranium were measured for each image and then multiplied by the slice thickness. To account for the gaps between slices, the mean area of the adjacent slices was calculated and then multiplied by the distance between the slices. Total cranial and PF volume were estimated by summing over all volumes.

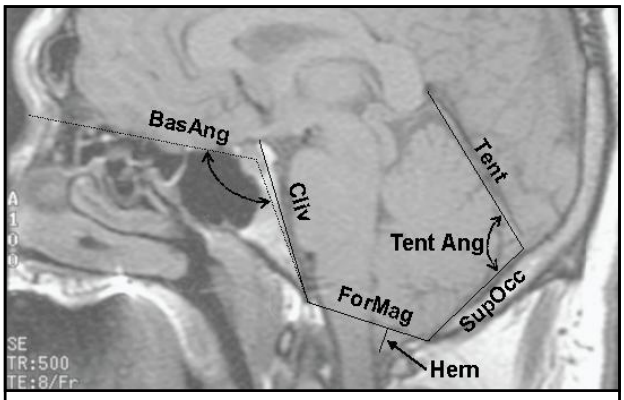

Figure 4. Cranial Morphology measurements. Hern = herniation; ForMag = foramen magnum; Tent = tentorium; SupOcc = supraoccipital bone; TentAng = tentorium angle; Cliv = clivus; BasAng = basal angle.

Table 1. Heritability of Cranial Morphologies

	h^2	p-value
Left herniation (mm)	0	0.5
Right herniation (mm)	0	0.5
Maximum herniation (mm)	0	0.5
Foramen magnum (mm)	0.19	0.274
Tentorium (mm)	0.11	0.309
Supraocciput (mm)	0.28	0.069
Tentorium angle (˚)	0.10	0.388
Clivus (mm)	0.39	0.054
Basal angulation (˚)	0.51	**0.014**
Posterior fossa volume (cc)	0.96	**0.004**
Cranial volume (cc)	0.11	0.324

h^2= heritability

Heritability was estimated for all cranial measurements using Sequential Oligogenic Linkage Analysis Routines 2.1.2 (SOLAR) (37). The polygenic command was used in SOLAR, which provides an estimate of the total additive genetic heritability. Basal angle and posterior fossa volume were significantly heritable ($p<0.05$) in the families. Although not significant by conventional standards, clivus and supraocciput measurements showed a trend towards significance ($p<0.10$).

Current CMI families

To date, we have ascertained 58 Caucasian families which meet our criteria for a qualitative linkage screen (338 individuals sampled, of those 156 are affected). Families were selected if they contained at least two sampled individuals affected with CMI with or without syringomyelia. Families were excluded if a family member was diagnosed with an associated disorder which is known to co-occur with Chiari and/or thought to cause an acquired form of CMI. These disorders include: Tethered Cord Syndrome, Pseudotumor Cerebri, Hydrocephalus, Marfan Syndrome, Ehlers-Danlos Syndrome, Spina Bifida, Crouzon Syndrome, Klippel-Feil, and Noonan Syndrome. Detailed family histories, medical records, and pre-operative MRI scans have been collected on a subset of these individuals. Current ascertainment efforts are focused on collecting this information for the remainder of individuals in these families, as well as ascertaining additional CMI families.

Power study

Using SIMLINK (38), I estimated the power for our study with the 58 families described above. SIMLINK estimates power for linkage using simulations. Known family structures, disease status, and sampling status are all provided as input. Model parameters used for the simulations ($N_{replicates}$=1,000) included: disease minor allele frequency (MAF) of 0.001, marker MAF of 0.30, low penetrance of 0.001, and an autosomal dominant mode of inheritance. An "affecteds-only" analysis was performed. If we assume a low recombination fraction (Θ=0 or 0.01), we have ~80% power to detect a LOD score of 3 or greater (Figure 5). Based on our simulations, our expected maximum LOD score is 4.46 (Θ=0).

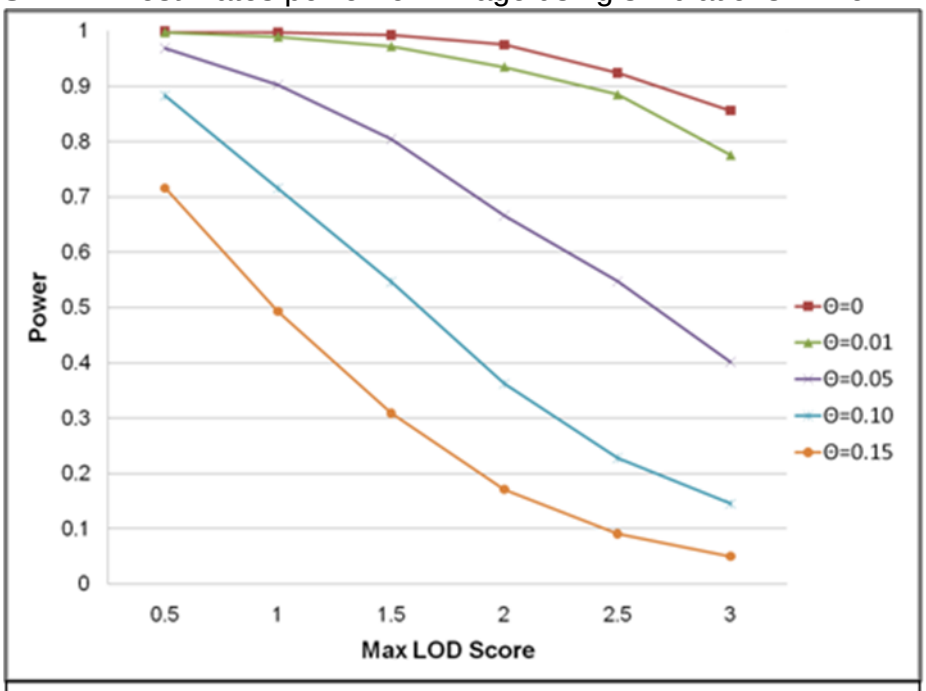

Figure 5. Power calculations using 58 multiplex families. Θ=Recombination fraction.

II. Preliminary Data for Specific Aim 2

Clustering CMI patients using clinical data

We compiled MRI measurements of the posterior fossa region (described above) on 25 unrelated, affected CMI patients. Cranial morphology measurements adjusted for age and sex (standardized residuals obtained from linear regressions) were used to cluster patients. All clustering was performed using GenePattern (39). Two clustering algorithms were used in combination with consensus clustering: 1) K-means clustering (40), and 2) Hierarchical clustering (41). Consensus clustering is a subsampling based method used to assess the stability of clusters and also aid in the identification of an optimal number of clusters (42). Different numbers of clusters (k=2-5) were

examined using each method. For each clustering method and value of k, a consensus matrix, M, was created where M(i,j) corresponds to the proportion of times patients i and j were present in the same cluster. A perfect consensus results in a matrix comprised only of zeros and ones (corresponding to dark blue and red, respectively, in a heatmap). Our primary objective was to assess the stability of our clusters given a sample size of only 25 and to look at the consistency across clustering algorithms.

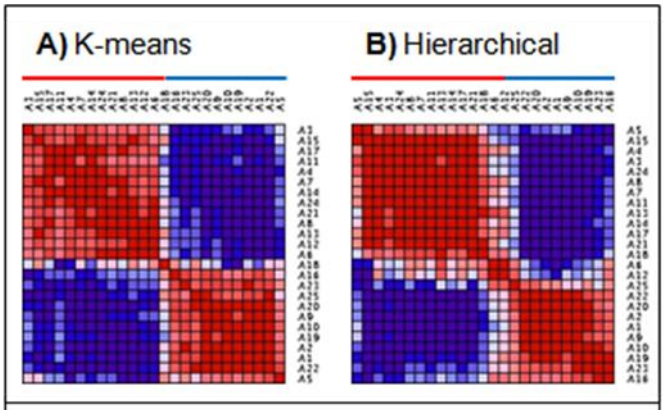

Figure 6. K-means and Hierarchical clustering in combination with consensus clustering (20 resampling iterations) were used to create consensus matrices for k=2(number of clusters). The red bar above each matrix corresponds to individuals belonging to class 1 and the blue bar corresponds to individuals belonging to class 2.

By evaluating the consensus matrices for k=2-5, we determined that k=2 was optimal for both methods. Results of the clustering analyses for k=2 are shown in Figure 6. As illustrated by the consensus matrices, we had fairly stable clusters regardless of the clustering algorithm used. In addition, only one individual was assigned to a different class using K-means versus Hierarchical clustering.

We wanted to further assess our clusters by comparing the mean PF measures between groups, as well as additional clinical features that we had collected on each patient. Our results suggest that the two classes obtained by clustering patients using PF measures are characterized by disease severity (Table 2). Class 1 is characterized by a more extensive tonsillar herniation, smaller supraoccipital bone, smaller PF volume, smaller PF volume / Total cranial volume and a greater number of patients who have undergone surgery. Although not significant, it appears that a greater number of patients with syringomyelia are present in class 1 versus class 2.

We are encouraged by our findings which suggest that with a sample size of 25 we are able to obtain fairly stable clusters that are not strongly dependent on the clustering method used and that are further validated by the small amount of clinical information we have collected. For Specific Aim 2, we will double our sample size and collect more information regarding clinical features of CMI, as well as biological information in the form of whole genome expression from both tissue and blood samples of CMI patients.

Table 2. Comparison of clinical features between classes.

Clinical Features	Class 1 (N=14)		Class 2 (N=11)		P-value†
	Mean	Std Dev	Mean	Std Dev	
Age	27.19	16.21	26.80	18.48	0.9558
Left Herniation	10.13	3.11	5.25	1.92	**0.0001**
Right Herniation	10.62	3.92	5.79	2.33	**0.0015**
Foramen Magnum	37.14	2.63	35.96	2.39	0.2581
Tentorium	51.97	4.03	51.37	4.30	0.7218
Supraoccipital	36.55	3.27	39.97	4.95	**0.0491**
Tentorial Angle	95.13	9.19	92.86	3.92	0.4151
Clivus	40.21	3.95	42.60	2.62	0.0982
Basal Angle	127.92	5.99	126.49	5.37	0.5414
PF Vol	184.82	19.73	213.79	27.34	**0.0053**
Total Vol	1380.40	115.65	1464.53	108.40	0.0764
PF Vol / Total Vol	0.13	0.01	0.15	0.01	**0.0098**
Disease‡					0.3542
Cer Ectopia	1	7.14%	2	18.18%	
CMI	8	57.14%	8	72.73%	
CMI/S	5	35.71%	1	9.09%	
Surgery‡					**0.0039**
Yes	11	78.57%	2	18.18%	
No	2	14.29%	3	27.27%	
Unknown	1	7.14%	6	54.55%	
Sex‡					1
Male	4	28.57%	3	27.27%	
Female	10	71.43%	8	72.73%	

Abbreviations: PF: Posterior Fossa; Vol: Volume; Cer Ectopia: Cerebellar Ectopia; CMI: Chiari Type I Malformation; S: Syringomyelia

CMI: 1 tonsil herniated ≥ 5 mm or both tonsils herniated ≥ 3 mm; Cer Ectopia: at least 1 tonsil herniated 2-4 mm

†P-values were obtained from T-tests and Fisher's exact tests for continuous and categorical variables, respectively.

‡Numbers refer to counts and percentages.

D. RESEARCH DESIGN AND METHODS

Table 3. Timeline.

	Project Year		
	1	2	3
Specific Aim 1: Qualitative Linkage Screen			
1a. Ascertainment and creation of clinical/radiographic dataset			
1b. Genotyping			
1c. Quality Control and Linkage Analyses			
Specific Aim 2: CMI Subtypes			
2a. Ascertainment and creation of clinical/radiographic dataset			
2b. RNA Extractions and Expression			
2c. Clustering analysis			

Specific Aim 1. To perform a qualitative linkage screen using multiplex CMI families. There are multiple lines of evidence supporting a genetic basis in at least a subset of nonsyndromic, CMI families. The identification of CMI susceptibility genes in even a small number of families may provide important information regarding the biological mechanisms which contribute to the development of CMI. Using 58 nonsyndromic, multiplex families, I, in collaboration with others, will conduct a genome-wide linkage screen to identify genomic regions likely to harbor CMI susceptibility genes. I will perform both a parametric and nonparametric linkage analysis since the underlying genetic model for CMI is unknown. If important clinical covariates are identified in Specific Aim 2, I will perform an Ordered-subset analysis to reduce the potential impact that heterogeneity across our families may have on our power to detect linkage. Regions showing significant evidence for linkage will be defined and prioritized for follow-up.

CMI Families

As described in the Preliminary Data section, we have ascertained 58 nonsyndromic, multiplex families meeting our inclusion criteria for a qualitative linkage screen. Over the next year, we will continue to expand our current families by sampling additional affected individuals, as well as collect new multiplex families. Together with others, I have recently developed a detailed questionnaire that will be given to both affected and unaffected family members. Questions concerning pregnancy history (e.g. birth trauma, environmental exposures), presence/absence of various associated conditions, symptom severity, surgical outcome, and family history of genetic syndromes that co-occur with CMI will be used to further characterize participants. We are in the process of re-contacting members from these 58 families to request that they complete this new questionnaire. In addition, we are collecting pre-operative MRIs from both affected and unaffected members of these families and any newly ascertained families. Blood samples will be collected from all willing participants.

Genotyping and Quality Control

Blood samples will be collected from participants in EDTA tubes. The DNA bank at the Duke Center for Human Genetics will extract DNA from the blood samples using the AutoPure LS® DNA extraction kit with Puregene® system reagents (Qiagen, Valencia, CA). A small amount of DNA will be run on an agarose gel to assess quality and the Picogreen fluorescent-dye assay (Molecular Dynamics) will be used to quantify the DNA. Individuals will be genotyped using Illumina

Human610-Quad BeadChips (San Diego, CA). The Human610 BeadChip holds four samples and contains over 610,000 tagging SNPs, including roughly 60,000 additional markers which target regions that are known or likely to contain copy number variation (CNV). Its average call rate and reproducibility exceed 99%. The protocol will be followed per the manufacturer's instructions. Briefly, genomic DNA will undergo whole-genome amplification, followed by fragmentation, hybridization to the bead chip which contains 50-mer probes, and single base extension with labeled nucleotides. Chips will be scanned using the iScan system (Illumina) in order to determine the genotypes.

Quality control (QC) procedures will be performed to ensure high quality data are used for analysis. Two family (1 male, 1 female) and two CEPH (1 male, 1 female) samples will be included across all sample plates in an alternating pattern and checked for mismatches. In addition, we will require call rates exceeding 98% for each individual and marker efficiency rates exceeding 98%. Markers with a MAF < 0.10 will be removed from all analyses. PEDCHECK (30) will be used to check for Mendelian inconsistencies and familial relationships will be verified using RELPAIR (31;32). I will also check for deviations from Hardy-Weinberg Equilibrium (HWE) using the Genetic Data Analysis program (GDA) (43). Initially, markers which show significant deviations ($p<0.0001$) from HWE will be removed from the analysis.

Qualitative Linkage Analysis

Merlin (44) will be used to perform all linkage analyses. Since the underlying genetic model for CMI is unknown, I will perform both parametric (model dependent) and nonparametric (model free) linkage analysis. For the parametric linkage analysis, I will assume a low penetrance of 0.001 (1 liability class: 0, 0.001, 0.001), an autosomal dominant mode of inheritance, and a rare disease allele frequency of 0.001. I will be performing an "affecteds-only" analysis where affected individuals contribute both phenotypic and genotypic information, while unaffected/unknown individuals contribute only genotypic information. This type of approach is necessary given the fact that very few "unaffected" members of our families have ruled out a diagnosis of CMI by MRI. In addition, data suggest that tonsillar herniation may not be a good indication for CMI (27), and use of such may result in phenotypic misclassification and lower power for our analysis. In addition to the standard LOD score, Merlin also provides estimates of the proportion of linked families (α) and the maximum heterogeneity LOD score (HLOD). HLOD is used to detect linkage, allowing for heterogeneity.

For the nonparametric linkage (NPL) analysis, I will use the S_{pairs} statistic, which assesses allele similarity across pairs of affected individuals, and the S_{all} statistic, which assesses allele similarity across subsets of affected individuals (34). Both allele-sharing statistics will be used since the power of each test tends to differ depending on the underlying genetic model (45). In addition, both the Kong and Cox linear and exponential model will be used (36). The exponential model is more suited for detecting a large increase in sharing over a small number of families, whereas the linear model performs best for detecting a small increase in sharing over a large number of families.

Both two-point (disease and one marker) and multipoint (disease and multiple markers) analyses will be performed. In order to perform the multipoint analysis, I will need to reduce the total number of SNPs. This will be accomplished by taking into account inter-marker LD, the genetic distance between SNPs, MAF, and marker heterozygosity. The final marker map should contain roughly 5,000 evenly spaced SNPs (Dr. Silke Schmidt, personal communication), with relatively high MAFs and heterozygosity. In order to maintain the correct type I error rate when conducting a multipoint analysis in families when one or both parents are missing, I will use the option, rsq, in Merlin which allows for the modeling of inter-marker LD between SNPs (46). This option groups SNPs into clusters based on an r^2 threshold. I will begin by grouping SNPs into clusters based on $r^2>0.16$, as suggested by Boyles, et al. (33). However, the current implementation of Merlin only

allows for clusters containing 10-20 markers, so if the threshold is set too low resulting in cluster sizes exceeding this level I will need to increase our threshold.

Once a linkage peak(s) has been identified, we will prioritize peaks with a maximum LOD of 3 or greater which are also supported by the two-point linkage analysis. The 1-LOD down support interval will be defined using multipoint peaks for future follow-up.

Follow-up approaches to the qualitative linkage screen

The decision to initially perform a qualitative linkage screen was based on power calculations performed for both a qualitative (Figure 5) and quantitative analysis using our 58 multiplex families. Power for a quantitative screen is currently limited by the number of cranial MRI scans that have been collected from family members. However, the use of quantitative traits as endophenotypes (e.g. PF volume) can be a very powerful approach for identifying disease loci. This approach can be especially useful when the affection status is not well defined, as is the case with CMI. As discussed earlier, we are actively requesting additional pre-operative MRI scans of the brain and spine from family members. In order to prepare for a future quantitative screen, which will ultimately be a more powerful approach, I, along with others, will take cranial morphology measurements from collected MRI scans, as well as estimate the heritability of each of the measurements.

Cranial morphology measurements from affected and unaffected individuals

Under the supervision of a board certified radiologist (Dr. David Enterline), I, along with another researcher, will take a series of cranial morphology measurements from the midline of a sagittal MRI (Figure 7), as well as measurements to estimate PF and cranial volume from a series of axial MRI scans. All measurements will be performed as described previously in the Preliminary Data section. Three additional measurements will also be taken. The tentorial opening, tentorium, occipital bone, foramen magnum, and clivus will be used as borders to calculate the posterior fossa (PF) area (Figure 7). In addition, we will measure posterior fossa height, which will be measured as the line extending from the top of the tentorium perpendicularly to the level of the foramen magnum. Boogaard angle (8) will be measured as the angle between the clivus and the foramen magnum. In addition, if MRI scans of the cervical and thoracic regions are available, we will look for the presence of a syrinx and, if present, will note the location (beginning and ending vertebra) and measure the diameter. We will also note if CSF flow studies are available to be later assessed by the neuroradiologist, Dr. Enterline.

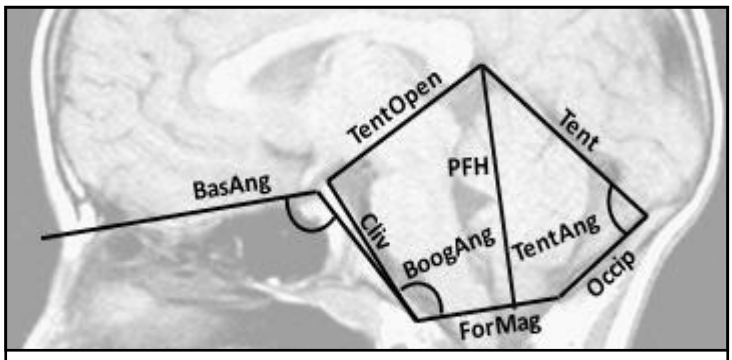

Figure 7. Cranial morphologies measured on a sagittal MRI. ForMag = foramen magnum; Occip = occipital; Tent = tentorium; TentOpen= tentorial opening; Cliv = clivus; PFH = posterior fossa height; TentAng = tentorium angle; BoogAng= Boogaard angle; BasAng = basal angle.

Heritabilities of Cranial Morphology Measurements

Heritabilities of all cranial morphology measurements described above will be estimated using SOLAR (37). Prior to analysis, all variables will be tested for normality using the SAS (Cary, NC) procedure, proc univariate. If necessary, variables will be transformed to approximate a normal distribution. The polygenic command will be used, which provides an estimate of the total additive genetic heritability. Heritability calculations will be performed for all measurements, while adjusting

for age and sex. In order to reduce the potential for ascertainment bias, I will correct for ascertainment by conditioning on the probands (37).

Ordered Subset Analysis

An additional approach to the follow-up of our linkage screen is to perform an Ordered-subset analysis (OSA) which can be used to reduce the impact of genetic heterogeneity across families (47). Families are ordered using a trait-related covariate to identify a subset of families which provide the greatest evidence for linkage. A permutation test is performed to assess the significance of the increased evidence for linkage provided by the subset. I will use information obtained in Specific Aim 2 to guide our selection of important covariates for OSA. Examples of family-level covariates which may be related to CMI include: mean age of onset, mean PF volume (adjusted for age and sex), and mean height of the clivus or supraoccipital bone (adjusted for age and sex).

Potential Limitations

Although our initial linkage and power study suggest that we will have sufficient power to identify a significant linkage peak, there is always the possibility that this will not occur. There are many reasons for this, including genetic heterogeneity, sample size, and misclassification of affected individuals. I am taking several approaches to reduce the impact of heterogeneity on the power for our study, including the use of HLOD, OSA, and strict inclusion criteria of the families included in the screen. In addition, at this point we will have recruited more multiplex families and additional family members which we will be able to include in the linkage analysis, thus increasing our sample size and power. After additional MRI scans have been collected, I will also reassess our power for a quantitative linkage screen using cranial morphology measurements that are determined to be both heritable and associated with disease status.

Specific Aim 2. To identify CMI subtypes using clinical and biological factors. Disease heterogeneity presents a major challenge to the study of any complex genetic disease. Although many individuals with Chiari are classified as having CMI, it is clear that a lot of variation exists in terms of the pattern and severity of symptoms, response to therapy, presence of associated conditions, age of onset, and the extent of tonsillar herniation. This variation is poorly understood and a more objective, sensitive method may be necessary in order to identify CMI subtypes. I will use both clinical and biological information separately to identify more homogeneous classes, or subtypes, in a cohort of 50 patients. Consistency with respect to the sets of subtypes would suggest a biological importance of the subtypes identified using clinical factors alone. However, we may find that biological features, such as gene expression patterns, may be necessary to identify biologically relevant subtypes which may not be readily observed using clinical features alone. Either result would provide important information regarding future identification and classification of CMI patients. Future work would also involve including these patients in a GWAS.

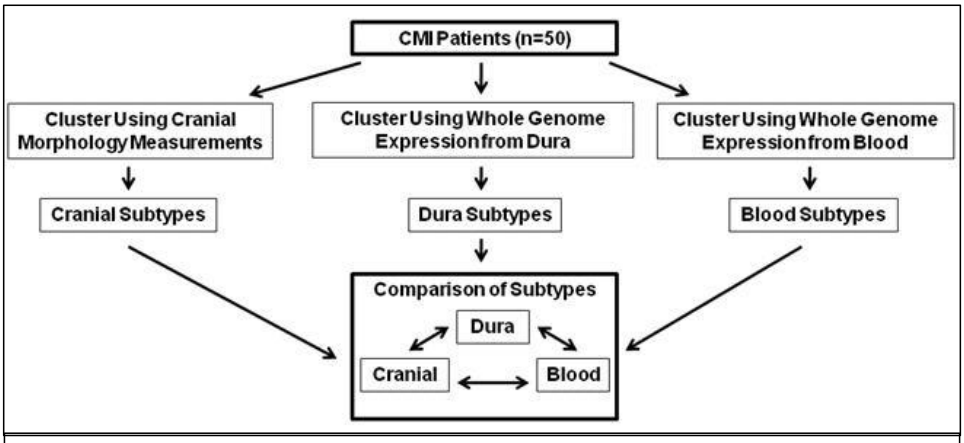

Figure 8. Outline of Specific Aim 2.

Patient cohort

Primary recruitment for this aim will occur through the Pediatric Neurosurgery Department at Duke University Medical Center. Patients of Dr. Herbert Fuchs and Dr. Gerry Grant will be enrolled in the study if they are diagnosed with CMI, scheduled to receive decompression surgery with duraplasty, and under the age of 18. Individuals will be excluded from the study if the child has/had a supratentorial or infratentorial tumor, lumbar shunt, significant history of birth trauma, history of any cervical or cranial surgery, or history of a myelomeningocele. It is standard practice for Dr. Fuchs to perform a craniectomy, duraplasty, and a C1 laminectomy if the CMI is severe enough to warrant surgery. Thus, based on the average number of surgeries performed per year, we expect to enroll a total of 50 patients for the study. We expect our study population to be comprised mostly of patients of Caucasian race and non-Hispanic ethnicity, with roughly equal numbers of males and females. All participating individuals will provide written informed consent that has been approved by Duke University's Institutional Review Board.

Participants will be asked to fill out a questionnaire to collect a basic family history and to assess pre-operative symptoms and the presence of associated conditions. Participants will also be asked to sign a release for their medical records, as well as brain and spinal MRIs, and pre- and post-operative CSF flow studies, if available. Sagittal and axial MRI scans from patients will be used to take a series of cranial morphology measurements, as described in Specific Aim 1.

Sample collection and processing

We anticipate collecting approximately fifty dura mater (5mmx5mm) and blood samples from Chiari decompression surgeries. Blood and dura mater samples will be collected from patients in PAXgene tubes and RNALater tubes (Qiagen, Valencia, CA), respectively, to prevent RNA degradation. We will extract RNA from the dura mater using the RNeasy Fibrous Tissue Mini kit (Qiagen, Valencia, CA), which I have previously tested on similar tissue types. Although we will only receive a ~5mmx5mm section of dura mater per patient, we are confident, based on previous studies (22;48;49), that we will be able to extract enough RNA for expression experiments. The PAXgene Blood RNA kit (Qiagen, Valencia, CA) will be used to extract RNA from the blood.

Whole genome expression

RNA extracted from both blood and dura mater will be quantified using the NanoDrop (ThermoScientific, Wilmington, DE) and, depending on the concentration, an RNA 6000 Pico Chip or Nano Chip (Agilent, Santa Clara, CA) will be used to assess quality. High quality RNA from blood and dura mater will be converted and amplified to generate labeled cRNA using Illumina® TotalPrep™ RNA Amplification Kits. The labeled cRNA will then be hybridized to the Illumina HT-12 v3 Expression BeadChips (San Diego, CA). The Illumina BeadChip holds twelve samples and

targets over 25,000 annotated genes with over 48,000 50-mer oligo probes. Chips will be scanned on an Illumina BeadArray reader. Initial pre-processing (background subtraction) and quality assessment of the gene expression data will be performed using the Gene Expression module from BeadStudio v3.2 (Illumina, San Diego, CA). Lumi (50) will be used to perform a model-based variance-stabilizing transformation followed by quantile normalization (51). An initial filtering step will be performed to remove probes with intensity values below background (Illumina detection p-value < 0.01), as well as probes with the least amount of variability (< 90th percentile of the coefficient of variability distribution).

Clustering of patients using clinical and biological factors

An unsupervised analysis will be performed to identify CMI subtypes. Clinical features consisting of MRI measurements of the PF region and biological features in the form of gene expression patterns will be used separately to cluster patients. To exclude the effects of age and sex on cranial morphology measurements and gene expression levels, I will regress the PF measures and expression levels on age and sex and consider only the standardized residuals. Although many clustering algorithms have been developed over the years, no single method appears superior in all situations. Thus, I will use two different methods to cluster CMI patients: 1) Hierarchical clustering, and 2) K-means clustering; each of which will be used in combination with consensus clustering. Agglomerative hierarchical clustering (bottom up) begins by assigning each patient (object) to its own cluster and then merging the two closest patients (41). This process is repeated until one large tree or group is formed, which can then be cut at different levels to produce varying numbers of clusters. While the number of clusters, k, does not need to be defined a priori for hierarchical clustering, it does need to be defined for K-means clustering. In its most basic form, K-means clustering begins by randomly selecting k objects to act as the initial cluster centroids or centers (40). Each object is then assigned to the cluster with which it is closest and the new cluster centers are determined. This process is repeated until convergence. Each of these clustering algorithms can be used in combination with consensus clustering, which is a subsampling based method that is used to assess the stability of clusters across several runs of a clustering algorithm, as well as to help identify an optimal number of clusters (42). Once each clustering algorithm has been run using all datasets and performed for a series of k values, I will look at the stability of the clusters derived from each method (for each k value), as well as the consistency across methods. Further information about the biology of this disorder can be obtained by identifying which genes or regulatory pathways differentiate these subtypes. Multiple t-tests (or ANOVA for subtypes > 2) will be used to compare the mean gene expression levels across subtypes. Using a p-value < 0.001 as our threshold for significance, I will identify which genes are significantly, differentially expressed across groups and follow-up with a pathway-based analysis using bioinformatics programs, such as WebGestalt (52) and David (53;54). Real-Time PCR will be used to validate five genes which are differentially expressed across clusters.

One of the primary goals of this aim is to determine whether clinical features alone can identify biologically relevant CMI subtypes, or whether biological features, such as gene expression patterns are necessary. To do this, I will first construct three matrices containing pairwise distances between patients using the clinical and gene expression data (blood and dura). As illustrated in Figure 8, the Mantel test will be used to test for correlation between each pairwise combination of distance matrices (e.g. correlation between the dural gene expression distance matrix and the clinical distance matrix) (55). Results from the Mantel test will allow us to assess whether patients with similar gene expression levels also have similar clinical features. In addition, I will compute the adjusted Rand index which provides a measure of agreement between two clustering outcomes (56). The Rand index will allow us to assess the similarity of subtypes/class memberships identified

through dural gene expression levels compared to those derived from clinical and blood gene expression data.

For simplicity, only cranial morphology measures obtained from MRI scans will be included in the initial clinical dataset. However, through our questionnaire we will obtain additional clinical information, including age of onset, duration of symptoms, presence/absence of a syrinx, syrinx diameter, syrinx location, presence/absence of various associated conditions (e.g. hydrocephalus, tethered cord syndrome, hereditary disorders of connective tissue, etc.), presence/absence of cranio-cervical bony abnormalities (e.g. platybasia, basilar invagination, etc.), hindbrain CSF flow findings (normal vs. abnormal), and a severity score for symptom classes (e.g. brainstem compression, upper cervical cord compression, etc) which will be derived from our questionnaire. Due to the mixed nature of the remaining clinical data, I will use an extension of the Mantel statistic which allows us to work in a regression framework. Distances calculated using the expression data will be used as the dependent variable, and distances calculated for each clinical covariate separately will be used as the independent variables (55). This regression model will be used to assess the relationship of each clinical covariate with the expression profiles.

Results from these analyses will provide us with further insight into the underlying biological features which may be driving the heterogeneity. We may also identify clinical covariates which are associated with these important biological features, and may be used to guide our linkage analysis in Specific Aim 1. Overall, this aim will provide us with information regarding both clinical and biological subtypes of CMI and the relationship between them.

Potential Limitations

One of the major limitations for this aim is that we may be unable to identify stable clusters using either the clinical or the gene expression data. This could be due to the sample size, or the fact that we have already reduced the clinical heterogeneity considerably by selecting only pediatric patients needing surgery. In addition, gene expression is known to vary both temporally and spatially, thus it is possible that in order for us to identify robust classes of patients we would need to look at a more relevant tissue type or at earlier stages in development. On the other hand, we may only be able to identify “stable” classes of patients using the gene expression data, suggesting that the combinations of clinical features alone are not sensitive enough to stratify the population. One goal of this aim is to use information about the underlying heterogeneity to help guide our analysis in Specific Aim 1 by potentially strengthening and refining our linkage peaks. However, Specific Aim 1 is not dependent on the success of this aim.

E. FUTURE DIRECTIONS

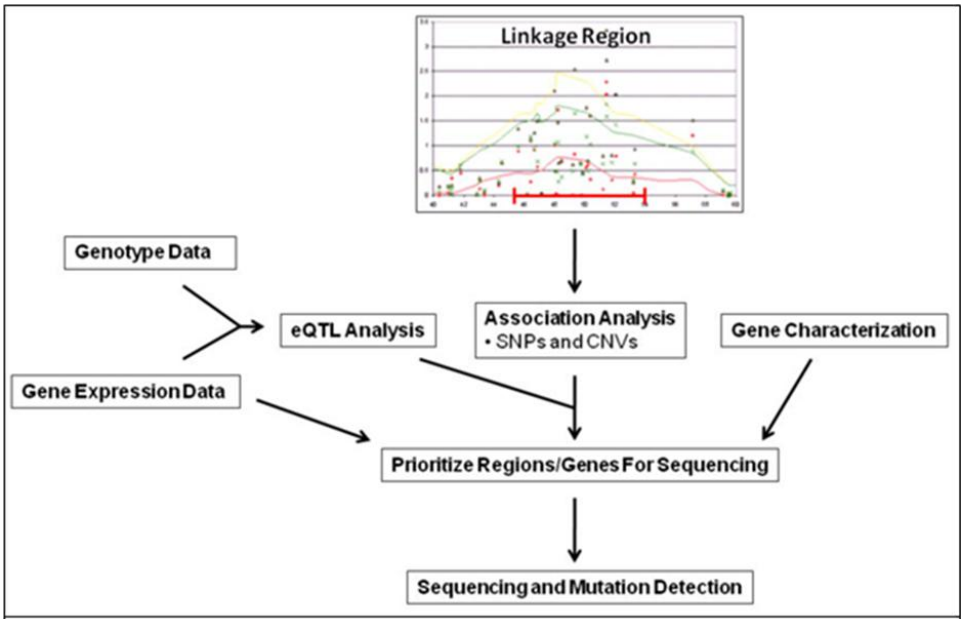

Figure 9. Follow-up of significant linkage peaks.

Fine-Mapping of Linkage Peaks and Copy Number Variant Detection

Throughout this study, we will continue to ascertain additional families that can be included during this stage of the project. Association analyses will be performed across each 1-LOD down support interval identified in Specific Aim 1. Prior to the analysis, the coverage provided by the Illumina 610 BeadChip will be assessed, although we expect it to provide adequate coverage for an initial screen. Qualitative association analyses (presence/absence of CMI) will be performed using the Pedigree Disequilibrium Test (PDT) (57) and the Genotype-pedigree Disequilibrium Test (geno-PDT) (58), both of which allow for extended families. We will also perform quantitative association analyses using measurements derived from cranial MRI scans, as described in Specific Aim 1. Measurements which are determined to be significantly heritable in our families will be tested for association with affection status using Generalized Estimating Equations (GEE), which controls for relatedness among individuals from the same family. Cranial morphology measurements which are both heritable and associated with affection status represent good candidate endophenotypes, or intermediate phenotypes of CMI. The software program, QTDT, will be used to test for association in our extended families (59). In order to adjust for multiple testing, the Benjamini-Hochberg false discovery rate (FDR) procedure will be used to correct for the number of SNPs evaluated across the interval (60). These association analyses are exploratory in nature, as they will be used in combination with other evidence to prioritize regions for re-sequencing. Thus, we will not be overly concerned if very few SNPs remain significant after our adjustment. If the association results provide no support for our regions of interest, it may be because CMI is caused by rare variants (private mutations) and our association analysis is unable to detect these. If this is the case, we will perform a haplotype analysis to further narrow our candidate intervals and then proceed with prioritizing regions for sequencing.

Raw signal intensities obtained from the Illumina Human610 BeadChips will be used to detect copy number variation (CNV) across our regions of interest. Illumina's Beadstudio will be used to convert raw signal intensities into log R ratios and B allele frequencies. These measures will be used in combination to detect CNVs. Since our study population consists of families, PennCNV (61) will be used to identify CNVs, as this method utilizes information from the family to

help define CNV boundaries, as well as classify CNVs as inherited or de novo. Once CNVs have been identified, we will use the feature in PennCNV which annotates CNVs based on nearby genes, overlapping exons, miRNAs, evolutionary conserved elements, and transcription factor binding sites. We will then test for association between each CNV and our qualitative and quantitative traits.

eQTL Analysis

DNA will be extracted from blood samples from our pediatric patient cohort described in Specific Aim 2 and be used for genotyping across Illumina Human610 BeadChips. An eQTL (expression quantitative trait loci) analysis will be performed since both whole genome expression and genotype data will be available from the same individuals. eQTL analysis tests for association between genotypes and expression levels. The analysis can be performed to test for both *cis*- and *trans*-regulatory SNP effects on expression. It is difficult to detect *trans*-eQTLs using a small sample size (62), so we will only test for *cis*-effects in our dataset. Results from this study could be used to help filter through and prioritize our association findings described above.

Selection of Candidate Genes/Regions for Sequencing

A variety of approaches will be used to prioritize regions /genes for sequencing. The significance of our association results, as well as the consistency across association analyses (qualitative and quantitative) will be examined. Results from the eQTL analysis can also be used to provide further support for the association results (ie: SNPs associated with both the disease phenotype and its respective gene's expression level). Known genes across the candidate regions will also be examined in order to identify biologically plausible candidates. Candidates would include genes known to be expressed at early stages in development, particularly in the cranial region, as well as genes known to be involved in the development of the occipital bone, and genes associated with known genetic syndromes that often co-occur with CMI. We will also look for crossover with our expression results.

Once we have prioritized our regions/genes for sequencing, we will assess how large the regions of interest are in order to determine the appropriate sequencing approach. If the regions are fairly small, we could use traditional Sanger sequencing on a moderate number of affected individuals from families which are linked to the region of interest. If the region is extensive, an exon capture array in combination with 2nd generation sequencing technologies will be considered for a small number of affected individuals.

F. BIBLIOGRAPHY

1. Milhorat TH, Chou MW, Trinidad EM, Kula RW, Mandell M, Wolpert C, Speer MC. Chiari I malformation redefined: clinical and radiographic findings for 364 symptomatic patients. Neurosurgery 1999 May;44(5):1005-17.

2. Mueller DM, Oro' JJ. Prospective analysis of presenting symptoms among 265 patients with radiographic evidence of Chiari malformation type I with or without syringomyelia. J.Am.Acad.Nurse Pract. 2004 Mar;16(3):134-8.

3. Speer MC, Enterline DS, Mehltretter L, Hammock P, Joseph J, Dickerson M, Ellenbogen RG, Milhorat TH, Hauser MA, George TM. Chiari type I malformation with or without syringomyelia: Prevalence and genetics. Journal of Genetic Counseling 2003 Aug 1;12:297-311.

4. Ellenbogen RG, Armonda RA, Shaw DWW, Winn HR. Toward a rational treatment of Chiari I malformation and syringomyelia. Neurosurg Focus 2000;8(3):1-10.

5. Schady W, Metcalfe RA, Butler P. The incidence of craniocervical bony anomalies in the adult Chiari malformation. J Neurol Sci 1987;82:193-203.

6. Milhorat TH, Bolognese PA, Nishikawa M, McDonnell NB, Francomano CA. Syndrome of occipitoatlantoaxial hypermobility, cranial settling, and chiari malformation type I in patients with hereditary disorders of connective tissue. J.Neurosurg.Spine 2007 Dec;7(6):601-9.

7. Tubbs RS, Elton S, Grabb P, Dockery SE, Bartolucci A, Oakes WJ. Analysis of the posterior fossa in children with the Chiari 0 malformation. Neurosurgery 2001;48:1050-5.

8. Bogdanov EI, Heiss JD, Mendelevich EG, Mikhaylov IM, Haass A. Clinical and neuroimaging features of "idiopathic" syringomyelia. Neurology 2004 Mar 9;62(5):791-4.

9. Meadows J, Kraut M, Guarnieri M, Haroun RI, Carson BS. Asymptomatic Chiari type 1 malformations identified on magnetic resonance imaging. J.Neurosurg. 2000;92:920-6.

10. Atkinson JLD, Kokmen E, Miller GM. Evidence of posterior fossa hyploplasia in the familial variant of adult Chiari I Malformation: case report. Neurosurgery 1998;42(2):401-4.

11. Stovner LJ, Cappelen J, Nilsen G, Sjaastad O. The chiari type 1 malformation in two monozygotic twins and first-degree relatives. Ann Neurol 1992;31:220-2.

12. Szewka AJ, Walsh LE, Boaz JC, Carvalho KS, Golomb MR. Chiari in the family: inheritance of the Chiari I malformation. Pediatr.Neurol. 2006 Jun;34(6):481-5.

13. Cavender RK, Schmidt JH, III. Tonsillar ectopia and Chiari malformations: monozygotic triplets. Case report. J.Neurosurg. 1995 Mar;82(3):497-500.

14. Speer MC, George TM, Enterline DS, Franklin A, Wolpert CM, Milhorat TH. A genetic hypothesis for Chiari Type I Malformation with or without Syringomyelia (CM1/S). Neurosurgical Focus 2000;8:1-4.

15. Batzdorf U. Treatment of syringomyelia associated with Chiari I Malformation. In: Tamaki T, Batzdorf U, Nagashima T, editors. Syringomyelia, Current Concepts in Pathogenesis and Management. Tokyo, Japan: Springer-Verlag; 2001. p. 121-35.

16. Levy WJ, Mason L, Hahn JF. Chiari Malformation Presenting in Adults - A Surgical Experience in 127 Cases. Neurosurgery 1983;12(4):377-90.

17. Dyste GN, Menezes AH, VanGilder JC. Symptomatic Chiari malformations. An analysis of presentation, management, and long-term outcome. J.Neurosurg. 1989 Aug;71(2):159-68.

18. Nakamura N, Iwasaki Y, Hida K, Abe H, Fujioka Y, Nagashima K. Dural band pathology in syringomyelia with Chiari type I malformation. Neuropathology 2000;1:38-43.

19. Arora P, Behari S, Banerji D, Chhabra DK, Jain VK. Factors influencing the outcome in symptomatic Chiari I malformation. Neurol.India 2004 Dec;52(4):470-4.

20. Shamir MH, Shilo Y, Fridman A, Chai O, Reifen R, Miara L. Sub-occipital craniectomy in a lion (Panthera leo) with occipital bone malformation and hypovitaminosis A. J.Zoo.Wildl.Med. 2008 Sep;39(3):455-9.

21. McCain S, Souza M, Ramsay E, Schumacher J, Hecht S, Thomas W. Diagnosis and surgical treatment of a Chiari I-like malformation in an African lion (Panthera leo). J.Zoo.Wildl.Med. 2008 Sep;39(3):421-7.

22. Cousins RJ, Eaton HD, Rousseau JE, Jr., Hall RC, Jr. Biochemical constituents of the dura mater in vitamin A deficiency. J.Nutr. 1969 Mar;97(3):409-18.

23. Marin-Padilla M, Marin-Padilla TM. Morphogenesis of experimentally induced Arnold-Chiari malformation. Journal of Neurological Sciences 1981;50:29-55.

24. Jiang X, Iseki S, Maxson RE, Sucov HM, Morriss-Kay GM. Tissue origins and interactions in the mammalian skull vault. Dev.Biol. 2002 Jan 1;241(1):106-16.

25. Warren SM, Longaker MT. The pathogenesis of craniosynostosis in the fetus. Yonsei Med.J. 2001 Dec;42(6):646-59.

26. Gagan JR, Tholpady SS, Ogle RC. Cellular dynamics and tissue interactions of the dura mater during head development. Birth Defects Res.C.Embryo.Today 2007 Dec;81(4):297-304.

27. Noudel R, Jovenin N, Eap C, Scherpereel B, Pierot L, Rousseaux P. Incidence of basioccipital hypoplasia in Chiari malformation Type I: comparative morphometric study of the posterior cranial fossa. J.Neurosurg. 2009 May 22.

28. Nishikawa M, Sakamoto H, Hakuba A, Nakanishi N, Inoue Y. Pathogenesis of Chiari malformation: a morphometric study of the posterior cranial fossa. J.Neurosurg. 1997 Jan;86(1):40-7.

29. Boyles AL, Enterline DS, Hammock PH, Siegel DG, Slifer SH, Mehltretter L, Gilbert JR, Hu-Lince D, Stephan D, Batzdorf U, et al. Phenotypic definition of Chiari type I malformation coupled with high-density SNP genome screen shows significant evidence for linkage to regions on chromosomes 9 and 15. Am.J.Med.Genet.A 2006 Dec 15;140(24):2776-85.

30. O'Connell JR, Weeks DE. PedCheck: a program for identification of genotype incompatibilities in linkage analysis. Am.J.Hum.Genet. 1998 Jul;63(1):259-66.

31. Boehnke M, Cox NJ. Accurate inference of relationships in sib-pair linkage studies. Am.J.Hum.Genet. 1997 Aug;61(2):423-9.

32. Epstein MP, Duren WL, Boehnke M. Improved inference of relationship for pairs of individuals. Am.J.Hum.Genet 2000 Nov;67(5):1219-31.

33. Boyles AL, Scott WK, Martin ER, Schmidt S, Li YJ, Ashley-Koch A, Bass MP, Schmidt M, Pericak-Vance MA, Speer MC, et al. Linkage disequilibrium inflates type I error rates in multipoint linkage analysis when parental genotypes are missing. Hum.Hered. 2005;59(4):220-7.

34. Whittemore AS, Halpern J. A class of tests for linkage using affected pedigree members. Biometrics 1994 Mar;50(1):118-27.

35. Gudbjartsson DF, Jonasson K, Frigge ML, Kong A. Allegro, a new computer program for multipoint linkage analysis. Nat.Genet. 2000 May;25(1):12-3.

36. Kong A, Cox NJ. Allele-sharing models: LOD scores and accurate linkage tests. Am.J.Hum.Genet. 1997 Nov;61(5):1179-88.

37. Almasy L, Blangero J. Multipoint quantitative-trait linkage analysis in general pedigrees. Am.J.Hum.Genet. 1998 May;62(5):1198-211.

38. Boehnke M. Estimating the power of a proposed linkage study: a practical computer simulation approach. Am.J.Hum.Genet. 1986;39:513-27.

39. Reich M, Liefeld T, Gould J, Lerner J, Tamayo P, Mesirov JP. GenePattern 2.0. Nat.Genet. 2006 May;38(5):500-1.

40. MacQueen J. Some methods for classification and analysis of multivariate observations. In: Cam LL, Neyman J, editors. Proceedings of the Fifth Berkeley Symposium on Mathematical Statistics and Probability. University of California Press; 1967. p. 281-97.

41. Eisen MB, Spellman PT, Brown PO, Botstein D. Cluster analysis and display of genome-wide expression patterns. Proc.Natl.Acad.Sci.U.S.A 1998 Dec 8;95(25):14863-8.

42. Monti S, Tamayo P, Mesirov J, Golub T. Consensus Clustering: A Resampling-Based Method for Class Discovery and Visualization of Gene Expression Microarray Data. Machine Learning 2003;52:91-118.

43. Zaykin D, Zhivotovsky L, Weir BS. Exact tests for association between alleles at arbitrary numbers of loci. Genetica 1995;96(1-2):169-78.

44. Abecasis GR, Cherny SS, Cookson WO, Cardon LR. Merlin--rapid analysis of dense genetic maps using sparse gene flow trees. Nat.Genet. 2002 Jan;30(1):97-101.

45. Shugart YY, Feng BJ, Collins A. The power and statistical behaviour of allele-sharing statistics when applied to models with two disease loci. J.Genet. 2002 Dec;81(3):99-103.

46. Abecasis GR, Wigginton JE. Handling marker-marker linkage disequilibrium: pedigree analysis with clustered markers. Am.J.Hum.Genet. 2005 Nov;77(5):754-67.

47. Hauser ER, Watanabe RM, Duren WL, Bass MP, Langefeld C.D., Boehnke M. Ordered subset analysis in genetic linkage mapping of complex traits. Genet Epidemiol. 2004;27(1):53-63.

48. Keller A, Ludwig N, Backes C, Romeike BF, Comtesse N, Henn W, Steudel WI, Mawrin C, Lenhof HP, Meese E. Genome wide expression profiling identifies specific deregulated pathways in meningioma. Int.J.Cancer 2009 Jan 15;124(2):346-51.

49. Greenwald JA, Mehrara BJ, Spector JA, Chin GS, Steinbrech DS, Saadeh PB, Luchs JS, Paccione MF, Gittes GK, Longaker MT. Biomolecular mechanisms of calvarial bone induction: immature versus mature dura mater. Plast.Reconstr.Surg. 2000 Apr;105(4):1382-92.

50. Du P, Kibbe WA, Lin SM. lumi: a pipeline for processing Illumina microarray. Bioinformatics. 2008 Jul 1;24(13):1547-8.

51. Lin SM, Du P, Huber W, Kibbe WA. Model-based variance-stabilizing transformation for Illumina microarray data. Nucleic Acids Res. 2008 Feb;36(2):e11.

52. Zhang B, Kirov S, Snoddy J. WebGestalt: an integrated system for exploring gene sets in various biological contexts. Nucleic Acids Res. 2005 Jul 1;33(Web Server issue):W741-W748.

53. Dennis G, Jr., Sherman BT, Hosack DA, Yang J, Gao W, Lane HC, Lempicki RA. DAVID: Database for Annotation, Visualization, and Integrated Discovery. Genome Biol. 2003;4(5):3.

54. Huang dW, Sherman BT, Lempicki RA. Systematic and integrative analysis of large gene lists using DAVID bioinformatics resources. Nat.Protoc. 2009;4(1):44-57.

55. Shannon WD, Watson MA, Perry A, Rich K. Mantel statistics to correlate gene expression levels from microarrays with clinical covariates. Genet.Epidemiol. 2002 Jun;23(1):87-96.

56. Yeung KY, Ruzzo WL. Principal component analysis for clustering gene expression data. Bioinformatics. 2001 Sep;17(9):763-74.

57. Martin ER, Monks SA, Warren LL, Kaplan NL. A test for linkage and association in general pedigrees: the pedigree disequilibrium test. Am J Hum Genet 2000 Jul;67:146-54.

58. Martin ER, Bass MP, Gilbert JR, Pericak-Vance MA, Hauser ER. Genotype-based association test for general pedigrees: the genotype-PDT. Genet Epidemiol 2003 Nov;25(3):203-13.

59. Abecasis GR, Cardon LR, Cookson WO. A general test of association for quantitative traits in nuclear families. Am J Hum Genet 2000 Jan;66(1):279-92.

60. Benjamini Y, Hochberg Y. Controlling the false discovery rate: a practical and powerful approach to multiple testing. J R Stat Soc B 1995;57:289-300.

61. Wang K, Chen Z, Tadesse MG, Glessner J, Grant SF, Hakonarson H, Bucan M, Li M. Modeling genetic inheritance of copy number variations. Nucleic Acids Res. 2008 Dec;36(21):e138.

62. Breitling R, Li Y, Tesson BM, Fu J, Wu C, Wiltshire T, Gerrits A, Bystrykh LV, de HG, Su AI, et al. Genetical genomics: spotlight on QTL hotspots. PLoS.Genet. 2008 Oct;4(10):e1000232.